Estimating Sulfur Content of Hydrogen Sulfide at Elevated Temperatures and Pressures Using an Artificial Neural Network Algorithm

ARTICLE *in* INDUSTRIAL & ENGINEERING CHEMISTRY RESEARCH · SEPTEMBER 2008

Impact Factor: 2.59 · DOI: 10.1021/ie8004463

2 AUTHORS:

Amir H. Mohammadi

557 PUBLICATIONS **4,821** CITATIONS

SEE PROFILE

Dominique Richon

Aalto University

533 PUBLICATIONS **6,599** CITATIONS

SEE PROFILE

CORRELATIONS

Estimating Sulfur Content of Hydrogen Sulfide at Elevated Temperatures and Pressures Using an Artificial Neural Network Algorithm

Amir H. Mohammadi and Dominique Richon*

Mines ParisTech, CEP/TEP-Centre énergetique et procédés, CNRS FRE 2861, 35 rue Saint Honoré, 77305 Fontainebleau, France

In this communication, we report an artificial neural network algorithm for estimating sulfur content of hydrogen sulfide at elevated temperatures and pressures. This model eliminates any need for characterization parameters, due to the tendency of sulfurs to react, required in thermodynamic models. To develop this algorithm, reliable experimental data reported in the literature on sulfur content of hydrogen sulfide are used. The developed model is then used to predict independent experimental data (not used in developing the model). It is shown that artificial neural network algorithm can be used as an efficient tool to estimate sulfur content of hydrogen sulfide.

1. Introduction

A serious problem in production of sour gases is precipitation of the sulfur in the formation, in well bores and in production facilities.[1] Sulfur deposition can cause a substantial and drastic reduction in the permeability of the formation near the wellbore. As the gas flows up the tubing string, the temperature and pressure are decreased causing further sulfur deposition. The occurrence of sulfur precipitation has also been reported when transporting natural gases.[2−4] A list of the most common places where sulfur deposition occurs in natural gas transportation and its impact on the equipment is given elsewhere.[4] To avoid sulfur deposition problems, accurate knowledge of sulfur + sour/acid gas phase behavior is important. One of the difficulties in describing the phase behavior of sulfur-containing systems is the lack of suitable characterization parameters as the tendency of sulfurs to react makes their characterization difficult. Furthermore, vapor and liquid phases of sulfur are composed of different molecules.[5−12] Sulfur may exist as a number of polymeric species ranging up to S_8 in the gas and combines with other gases to produce polysulfides or sulfanes such as H_2S_9.[13,14] The amount of each molecule depends both on pressure and temperature.[9−12] Sulfur vapors are mainly composed of light sulfur molecules (typically S_2-S_8) around the critical point; whereas the most abundant vapor sulfur species below 400 K and at saturation pressure seem to be S_8.[5−12,15,16] Under atmospheric pressure and at temperatures greater than the fusion temperature, liquid sulfur is composed of about 99% of S_8 and traces of lighter molecules.[9−12,16] Nevertheless, if temperature increases, the ring molecules of sulfur polymerize. Liquid sulfur begins to polymerize at about 430 K.[9−12,17] Two thermodynamically stable forms of solid sulfur can also exist. If liquid sulfur is slightly cooled, it becomes monoclinic sulfur (or β sulfur) at fusion temperature. If monoclinic sulfur is cooled again, it converts into orthorhombic sulfur (or α sulfur).[9−12,17] On the other hand, it has been argued that when transporting natural gas, the solubility of sulfur is very low. Although the composition of natural gas when transported can vary according to its origins, sulfur's solubility under transportation conditions does not greatly differ with gas composition. This can partially be explained by the fact that after natural gas treatment, the amount of hydrogen sulfide, which greatly influences the sulfur solubility, is very low.[9−12] Modeling sulfur + sour/acid gas phase equilibrium by conventional thermodynamic models clearly requires the use of many unknown parameters considering the above-mentioned reactions should be taken into account in the thermodynamic model.

Artificial neural network (ANN) algorithms are known to be effective in modeling complex systems. These models have large numbers of computational units connected in a massively parallel structure and do not require an explicit formulation of the mathematical or physical relationships of the handled problem.[18] Therefore, these can be regarded as an alternative method for the estimation of sulfur content of sour/acid gases. The ANNs are first subjected to a set of training data consisting of input data together with corresponding outputs. After a sufficient number of training iterations, the neural network learns the patterns in the data fed to it and creates an internal model, which it uses to make predictions for new inputs.

The aim of this work is to indicate the capability of the ANN algorithm for estimating the sulfur content of hydrogen sulfide. Among various ANNs reported in the literature, the feed-forward (back-propagation) neural network (FNN) algorithm is used, which is known to be effective in representing the nonlinear relationships between variables in complex systems and can be regarded as a large regression method between input and output variables.[22] The optimization algorithm chosen in this work is a modified Levenberg−Marquardt algorithm[18−21] with the Bayesian regularization technique, which is specially indicated to optimize ANNs using a small learning sample size. The reliable experimental data reported in the literature are used to develop and then validate this model. For this purpose, a review is first made on the existing experimental data and thermodynamic models reported in the literature.

2. Literature Review

Many experimental and theoretical studies have been done for the estimation of sulfur content in gases. This review covers a brief description of the experimental results and proposed models. Some parts of the materials in this section are based

* To whom correspondence should be addressed. E-mail: richon@ensmp.fr. Tel.: +(33) 1 64 69 49 65. Fax: +(33) 1 64 69 49 68.

10.1021/ie8004463 CCC: $40.75
Published on Web 09/26/2008

Table 1. Literature Review of Experimental Data for Sulfur Content of Various Gases

author (s)	system	temp range (K)	pressure range (MPa)	remarks
Sun and Chen[33]	seven (CH_4 + H_2S + CO_2) ternary mixtures	303−363	20−45	The mole fraction of H_2S in sour gas mixture ranged from 0.0495 to 0.2662 and that of CO_2 ranged from 0.0086 to 0.1039
Migdisov et al.[32]	gaseous hydrogen sulfide	323−563	up to 20	
Gu et al.[31]	two rich-H_2S natural gases	363	up to 34.7 and 32.8	The mole fractions of H_2S were 0.4411 and 0.9509
	pure H_2S, pure CO_2 and pure methane	363 (for the solubility of sulfur in pure H_2S) 363 and 383 (for the solubility of sulfur in pure CO_2) and 383 (for the solubility of sulfur in pure methane)	up to 36.2 (for the solubility of sulfur in pure H_2S) up to 40.5 (for the solubility of sulfur in pure CO_2) and up to 50.2 (for the solubility of sulfur in pure methane)	
Davis et al.[30]	sour gases	333, 363, 393, and 423 K	5−55	high hydrogen sulfide content (up to 90%)
Brunner et al.[28]	sour gas mixtures of various compositions	394−486	up to 155	
Brunner and Woll[25]	pure hydrogen sulfide and four gas mixtures composed of H_2S, CO_2, CH_4, and N_2	373−433	up to 60	
Swift et al.[27]	hydrogen sulfide	390−450	35−140	
Roof[24]	hydrogen sulfide	317−394	up to 31	
Kennedy and Wieland[23]	pure methane, carbon dioxide, hydrogen sulfide, and mixtures of these gases	339, 367, and 394	6.9−41.3	

on those reported by Karan et al.[14] for experimental studies and Serin et al.[9−12] for theoretical works:

Most of the reported experimental data on the solubility of sulfur in sour/acid gases are in the high temperature ranges, typically above 373.15 K. Kennedy and Wieland[23] measured the equilibrium sulfur content of pure methane, carbon dioxide, hydrogen sulfide, and mixtures of these gases at temperatures of 339, 367, and 394 K and in the pressure range of 6.9−41.3 MPa. Roof[24] measured solubility of sulfur in hydrogen sulfide in the range of temperature between 317 and 394 K and at pressures up to 31 MPa. These results differed significantly from those of Kennedy and Wieland,[23] and it seems the experimental approach used by Kennedy and Wieland[23] is questionable.[9−12,16,25,26] Serin et al.[9−12] also tried to recalculate the results of Kennedy and Wieland;[23] however, it was impossible to correctly represent the evolution of solid sulfur's solubility when under pressure.

Swift et al.[27] reported the solubility of sulfur in hydrogen sulfide at pressures of 35−140 MPa and in a temperature range of 390−450 K, conditions that may be encountered in high-pressure natural gas reservoirs. Brunner and Woll[25] measured the sulfur solubility in pure hydrogen sulfide and in four gas mixtures composed of H_2S, CO_2, CH_4, and N_2 in a temperature range of 373−433 K and at pressures up to 60 MPa. Their solubility data in hydrogen sulfide were in good agreement with those reported by Swift et al.[27] and by Roof.[24] Furthermore, the figures given by Roof[24] for the range of up to 25 MPa agree with the results of Brunner and Woll[25] but deviate at higher pressures in the direction of lower solubilities.[25]

Later, Brunner et al.[28] measured the sulfur solubility in sour gas mixtures of various compositions at pressures up to 155 MPa and in the temperature range of 394−486 K. One of their objectives was to study the effect of alkanes up to carbon number six. Woll[29] examined the effect of hydrogen sulfide on the depression of the freezing point of sulfur. Davis et al.[30] of Alberta Sulfur Research Limited (ASRL) have reported solubility data in sour gases of high hydrogen sulfide content (up to 90%) at four temperatures of 333, 363, 393, and 423 K and

Table 2. Thermodynamic Models Concerning Gas Production and Transportation Conditions

thermodynamic models concerning gas production conditions	thermodynamic models concerning gas transportation conditions
Sun and Chen[33]	Serin et al.[9−12]
Heideman et al.[16]	Pack[4]
Karan et al.[14]	Wilkes and Pareek[3]
Gu et al.[31]	
Tomcej et al.[26]	

over a pressure range of 5−55 MPa. Gu et al.[31] measured the solubility of sulfur in two rich-H_2S natural gases at 363 K, where the mole fractions of H_2S were 0.4411 and 0.9509, respectively, and the pressures were up to 34.7 and 32.8 MPa, respectively. Gu et al.[31] also measured solubility of sulfur in pure H_2S at 363 K and pressures up to 36.2 MPa, pure CO_2 at 363 and 383 K at pressures up to 40.5 MPa, and pure methane at 383 K and pressures up to 50.2 MPa. Migdisov et al.[32] carried out experiments for solubility of sulfur in gaseous hydrogen sulfide in the H_2S−S system at temperatures between 323 and 563 K and pressures up to 20 MPa. Sun and Chen[33] measured solubility of elemental sulfur in seven (CH_4 + H_2S + CO_2) ternary mixtures with a temperature-range of 303−363 K and a pressure-range of 20−45 MPa. The mole fraction of H_2S in sour gas mixture ranged from 0.0495 to 0.2662 and that of CO_2 ranged from 0.0086 to 0.1039. Table 1 summarizes the literature review of experimental data for sulfur content of various gases.

Modeling of sulfur solubility has also been the subject of many studies: The various models described by the authors used typically the Peng−Robinson equation of state (PR-EoS).[34] Since it is known that sulfur deposits normally occur during gas production, models present in the literature concern ranges of pressure, temperature, and hydrogen sulfide amounts, which are greater than those of gas transportation conditions.

Tomcej et al.[26] used sulfur's experimental critical temperature and pressure to describe sulfur's behavior. They succeeded in correlating the experimental data at pressures ranging from 8 to 69 MPa and at temperatures ranging from 305 to 480 K for

Table 3. Experimental and Calculated/Predicted Sulfur Content of Hydrogen Sulfide (Mass %) Using ANN Algorithm

	sulfur content of hydrogen sulfide/mass %					
author (s)	T (K)	P (MPa)	experimental value	calculated/ predicted value	AD %[a]	D %[b]
Roof[24c]	316.3	7.028	1.24	1.26	1.7	−1.7
	316.3	10.473	1.37	1.42	3.7	−3.7
	316.3	17.363	1.47	1.54	4.9	−4.9
	316.3	24.253	1.54	1.62	4.7	−4.7
	316.3	31.143	1.63	1.64	0.6	−0.6
	338.7	7.028	1.94	1.61	17.1	17.1
	338.7	10.473	2.16	2.16	0.0	0.0
	338.7	17.363	2.70	2.67	1.1	1.1
	338.7	24.253	3.07	3.08	0.4	−0.4
	338.7	31.143	3.29	3.25	1.2	1.2
	366.5	10.473	2.68	2.30	14.3	14.3
	366.5	17.363	4.44	4.00	9.7	9.7
	366.5	24.253	5.84	5.82	0.3	0.3
	366.5	31.143	6.92	6.67	3.6	3.6
	374.8	10.473	2.03	1.91	5.9	5.9
	374.8	17.363	4.27	3.97	7.0	7.0
	374.8	24.253	5.82	6.44	10.6	−10.6
	374.8	31.143	7.23	7.64	5.8	−5.8
	383.2	17.363	3.98	3.61	9.2	9.2
	383.2	24.253	5.85	6.73	15.0	−15.0
	383.2	31.143	7.11	8.35	17.4	−17.4
Brunner and Woll[25]	373.15	10	1.79	2.00	11.9	−11.9
	373.15	10	2.16	2.00	7.3	7.3
	373.15	12	2.58	2.93	13.5	−13.5
	373.15	18	4.67	5.16	10.6	−10.6
	373.15	30	7.46	7.47	0.1	−0.1
	373.15	30	7.57	7.47	1.4	1.4
	373.15	40	8.94	8.51	4.8	4.8
	373.15	50	10.8	9.44	12.6	12.6
	393.15	12	1.35	1.58	17.0	−17.0
	393.15	15	2.43	2.82	16.0	−16.0
	393.15	15	2.70	2.82	4.4	−4.4
	393.15	20	4.47	4.52	1.1	−1.1
	393.15	32	8.48	8.67	2.3	−2.3
	393.15	40	9.96	10.73	7.7	−7.7
	393.15	51	12.60	12.58	0.2	0.2
	393.15	60	15.60	14.18	9.1	9.1
	413.15	15	1.42	1.25	12.2	12.2
[c]	413.15	24	4.92	4.82	2.1	2.1
	413.15	24	4.98	4.82	3.3	3.3
	413.15	33	8.97	7.68	14.4	14.4
	413.15	40	10.92	10.78	1.3	1.3
	413.15	40	10.95	10.78	1.6	1.6
	413.15	44	11.70	10.78	7.9	7.9
	413.15	50	13.40	13.68	2.1	−2.1
	413.15	60	16.50	16.15	2.1	2.1
	433.15	15	1.06	1.07	0.9	−0.9
	433.15	19.6	2.14	2.23	4.2	−4.2
	433.15	24	4.38	4.28	2.3	2.3
	433.15	24	4.48	4.28	4.5	4.5
	433.15	30	6.69	7.25	8.3	−8.3
	433.15	30	6.88	7.25	5.3	−5.3
	433.15	40	10.70	10.75	0.4	−0.4
	433.15	40	11.10	10.75	3.2	3.2
	433.15	45	13.10	14.20	8.4	−8.4
	433.15	52	15.00	14.20	5.3	5.3
	433.15	60	17.20	17.17	0.2	0.2
	433.15	60	17.60	17.17	2.5	2.5
Gu et al.[31d]	363.2	11.83	3.53	3.14	11.0	11.0
	363.2	14.79	3.70	3.94	6.3	−6.3
	363.2	19.14	5.25	4.74	9.8	9.8
	363.2	25.86	5.76	5.52	4.2	4.2
	363.2	31.03	6.75	6.25	7.4	7.4
	363.2	36.21	7.42	6.91	7.0	7.0

[a] AD: Absolute deviation = (experimental value-predicted/calculated value)/experimental value. [b] D: Relative deviation = (experimental value-predicted/calculated value)/exp experimental value. [c] Data were used for training (and testing). [d] Data were used for validation.

mixtures covering the entire hydrogen sulfide range. They were able to fit the experimental data reported by Roof,[24] Brunner and Woll,[25] Woll,[29] and Brunner et al.[28] Nevertheless, they used

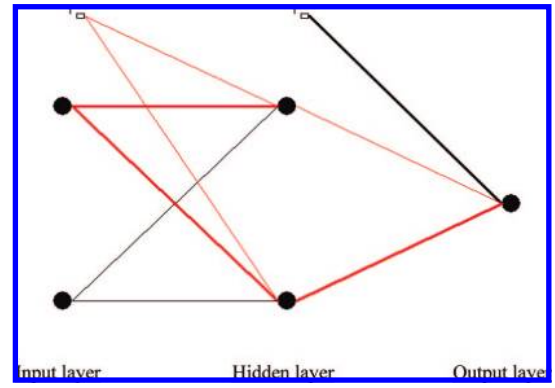

Figure 1. Architecture of the neural network algorithm for estimating sulfur content of H_2S: (1) bias, (●) neuron, (output neuron) logarithm of sulfur content (in mass fraction) of H_2S; (input neurons) T/273.15 and logarithm of pressure (pressure in MPa).

Table 4. Number of Neurons, Hidden Layers, Parameters, Data, and Type of Activation Function Used in This Algorithm[a]

layer	number of neurons
1	2
2	2
3	1

[a] Number of hidden layers = 1; number of parameters = 9; number of data used for training (and testing) = 58; number of data used for validation = 6; type of activation function = tangent sigmoid.

the experimental coordinates of sulfur which correspond to the lighter molecules of sulfur, whereas in the experimental conditions the most abundant sulfur specie is S_8.

Swift et al.[27] developed a reaction equilibrium model to interpret and extrapolate sulfur solubility data. Extrapolation to temperatures above the range of the experimental data can be done with reasonable confidence using the model.

Gu et al.[31] proposed empirical critical coordinates for the S_8 molecule. These parameters were determined from the regression of the vapor pressure to lower temperatures. The authors also modified van der Waals mixing rules for the repulsive term. They added two adjusted parameters for repulsive term calculations. Therefore, they had three parameters (two for repulsive term calculations and one for attractive term calculations) to fit a maximum of seven experimental points for each binary. Moreover, these three parameters depend on the temperature, and their evolution appears to be complex.

Karan et al.[14] and Heideman et al.[16] regressed the attractive and repulsive parameters of PR-EoS[34] for the S_8 species from the vapor pressure and liquid density data of pure sulfur. Equilibrium reactions between the sulfur molecules, which constitute sulfur vapors and reactions that lead to the formation of polysulfanes are considered. For the products (S_7 to S and H_2S_2 to H_2S_9), the EoS attractive and repulsive parameters are calculated from the so-called source species. The repulsive parameter for S_8 is taken as a constant and the attractive parameter for S_8 has a particular expression. This model is particularly suitable for describing liquid and vapor sulfur behaviors due to the temperature range used to determine the attractive parameter for S_8. Moreover, it was not taken into account that sulfur could polymerize in liquid phase.

Furthermore, in the model of Heideman et al.,[16] eight sulfur species ranging from S_1 to S_8 are fully accounted. When hydrogen sulfide is a mixture component, equilibrium formation of the sulfanes from H_2S_2 to H_2S_9 is included, as is the dissociation of hydrogen sulfide to produce molecular hydrogen. The PR-EoS[34] is used to describe the fluid phases, as was done

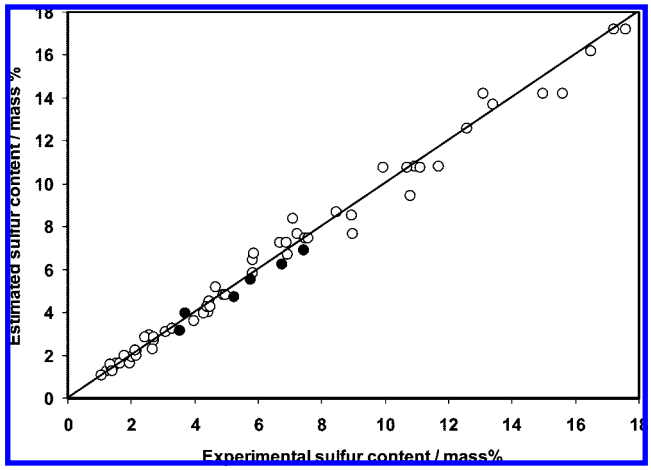

Figure 2. Estimated sulfur content of hydrogen sulfide (mass %) versus corresponding experimental value (mass %): (○) data used for training (and testing); (●) data used for validation.

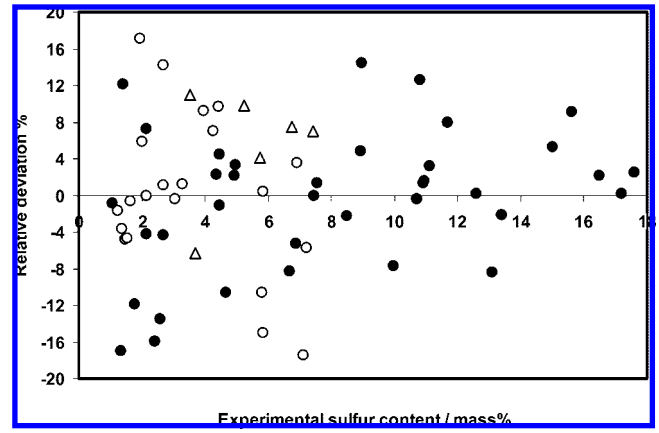

Figure 3. Relative deviation between estimated sulfur content of hydrogen sulfide (mass %) and corresponding experimental value (mass%) versus experimental value for sulfur content of hydrogen sulfide (mass%): (○) Roof;[24] (●) Brunner and Woll;[25](△) Gu et al.[31]

by Karan et al.[14] However, chemical reaction equilibria determine the distribution of the sulfur between the various possible species in all of the fluids. The vapor- and liquid-phase nonidealities are accounted for through the equation of state. A separate model is employed for solid sulfur, which is treated as S_8. The model is complex as it is but does not consider the possibility of more than one isomer of any of the S_n species. The well-known existence of two different crystalline forms of sulfur was also not taken into account.[16]

Sun and Chen[33] used a similar model of Gu et al.[31] The three binary interaction parameters were adapted from the experimental data sets. Contrary to Gu et al.,[31] the three parameters are considered to be temperature independent. However, the possible chemical reactions were not taken into account by them.

The above authors tried to model sulfur's solubility under the production conditions. Other authors tried to predict the values of sulfur solubility under natural gas transportation. Wilkes and Pareek[3] and Pack[4] used two different process simulation packages and neither explained the equations nor the data used to obtain their predictions. Furthermore, the chemical reactions were not considered. Serin et al.[9−12] proposed a flash model to calculate sulfur's solubility under the condition of natural gas transportation. The equations are the equality of the fugacities and the possible reactions involving sulfur and partial mass balances. The PR-EoS[34] is chosen with van der Waals mixing rules, with two binary interaction parameters, of which one of the two is temperature dependent. However, because experimental data are not readily available, the van der Waals mixing rules with one binary interaction parameter, which is temperature dependent, was selected. It was assumed that sulfur is mainly composed of the S_8 species under natural gas transportation conditions, and pseudocritical parameters for this molecule were determined. A new way was proposed to express the fugacity of pure solid sulfur, which links it to the pure liquid fugacity at fusion temperature under atmospheric pressure. Table 2 summarizes thermodynamic models concerning gas production and transportation conditions.

3. Feed-Forward Neural Network Algorithm

Feed-forward neural networks are the most frequently used ANN, which are designed with one input layer, one output layer, and hidden layers.[35−38] The number of neurons in the input and output layers is equal to the number of inputs and outputs, respectively.[35−38] The accuracy of model representation depends on the architecture and parameters of the neural network.[35−38] In the FNN algorithm, the input layer of the network receives all the input data and introduces scaled data to the network.[38] The data from the input neurons are propagated through the network via weighted interconnections.[38] Every i neuron in a k layer is connected to every neuron in adjacent layers.[38] The i neuron within the hidden k layer performs the following tasks: summation of the arriving weighted inputs and propagations of the resulting summation through an activation function, f, to the adjacent neurons of the next hidden layer or to the output neuron(s). In this work, the activation function, f, is tangent sigmoid:

$$f(x)=\frac{1-e^{-x}}{1+e^{-x}} \qquad x\in[-\infty,+\infty] \text{ and } f(x)\in[-1,+1] \tag{1}$$

where x stands for parameter of activation function. A bias term, b, is associated with each interconnection in order to introduce a supplementary degree of freedom. The expression of the weighted sum, S, to the i^{th} neuron in the k^{th} layer ($k \geq 2$) is[38]

$$S_{k,i}=\sum_{j=1}^{N_{k-1}}[(w_{k-1,j,i}I_{k-1,j})+b_{k,i}] \tag{2}$$

where w is the weight parameter between each neuron-neuron interconnection and $I_i=[I_{i,1},\ldots,I_{i,N_{k-1}}]$ represents input vector. Using this feed-forward network with tangent sigmoid activation function, the output, O, of the i neuron within the hidden k layer is

$$O_{k,i}=\frac{1-\exp\left(-\sum_{j=1}^{N_{k-1}}[(w_{k-1,j,i}I_{k-1,j})+b_{k,i}]\right)}{1+\exp\left(-\sum_{j=1}^{N_{k-1}}[(w_{k-1,j,i}I_{k-1,j})+b_{k,i}]\right)} \tag{3}$$

The Levenberg−Marquardt algorithm[18−21] consists in modifying the network's weight by the following equations:

$$w_j=w_{j-1}-[\bar{H}+\mu_j\bar{I}]^{-1}\nabla J(w_{j-1}) \tag{4}$$

with

$$\bar{H}=\sum_{k=1}^{n}\left(\frac{\partial \mathrm{err}^k}{\partial w_j}\right)^T+\sum_{k=1}^{n}\left(\frac{\partial^2 \mathrm{err}^k}{\partial w_j\,\partial w_j^T}\mathrm{err}^k\right) \tag{5}$$

where err^k, μ, J, N, $\bar{H}$ and $\bar{I}$ are the residue vector, the step

values of the Levenberg−Marquardt algorithm,[18−21] the Jacobian matrix of the first derivative of global error to weight, the number of feed inputs, Hessian matrix, and identity matrix, respectively. The valule err^k is defined by

$$err^k = (\text{experimental value}) - (\text{calculated value}) \quad (6)$$

To develop the ANN, the data sets are generally subdivided into three groups corresponding to the following three steps: training, testing, and validation.[38] After partitioning the data sets, the training set is used to adjust the parameters. All synaptic weights and biases are first initialized randomly. The network is then trained; its synaptic weights are adjusted by the optimization algorithm, until it correctly emulates the input/output mapping, by minimizing the average root-mean-square error.[38] The testing set is used during the adjustment of the network's synaptic weights to evaluate the algorithms performance on the data not used for adjustment and stop the adjusting if the error on the testing set increases. Finally, the validation set measures the generalization ability of the algorithm after the fitting process.[38]

4. Results and Discussion

As mentioned earlier, the experimental data of Kennedy and Wieland[23] are questionable.[9−12,16,25,26] Therefore, these data were eliminated from our study. The experimental data of Migdisov et al. [32] were also not considered in our study, because it seems these data at high temperatures are not very reliable. Therefore, we only considered the experimental data reported in Table 3 for developing the ANN algorithm. As can be observed, this table reports sulfur content of hydrogen sulfide in the temperature range of (316−433) K and pressures up to 60 MPa. The ANN algorithm shown in Figure 1 and detailed in Table 4 with one hidden layer was devoted to compute the logarithm of sulfur content (in mass fraction) of H_2S (output neuron) in function of temperature/273.15 and logarithm of pressure (input neurons), which gives the lowest number of hidden neurons. The optimum number of neurons in the hidden layer according to both the accuracy of the fit (minimum value of the objective function) and the predictive power of the neural network was found to be 2. Table 3 and Figures 2 and 3 compare the results of the ANN algorithm with the experimental data.[24,25,31] As can be seen, acceptable agreement was achieved and the average absolute deviation among all the experimental and calculated/predicted data is 6.1%. The maximum absolute deviation (AD) among all the experimental and calculated /predicted data is less than 18%. To better present the deviations, we have compared relative deviations between estimated sulfur content of hydrogen sulfide and corresponding experimental value versus experimental value for sulfur content of hydrogen sulfide in Figure 3. As can be observed, high deviations are observed at low values of sulfur content of hydrogen sulfide. Considering the fact that such measurements, especially at high temperatures and high pressures and low sulfur contents, are indeed not easy and some experimental data may have errors, the AD up to 18% can be regarded acceptable. It should be mentioned that the ANN algorithm introduced in this study was developed using the most reliable experimental data found in the literature on sulfur content of hydrogen sulfide. By generating reliable experimental data on sulfur content of hydrogen sulfide in the future and readjusting the model parameters, more reliable predicted data would be expected.

5. Conclusions

A review was made on the existing experimental data and thermodynamic models reported in the literature for estimating sulfur content of gases. The review showed a need to generate reliable experimental data and an alternative tool to model sulfur content. A feed-forward artificial neural network algorithm was then developed to estimate sulfur content of hydrogen sulfide in the temperature range of 316−433 K and pressures up to 60 MPa. The model was developed using the most reliable experimental data found in the literature. The agreements between the experimental and calculated/ predicted data were generally found acceptable.

Literature Cited

(1) Hyne, J. B. Controlling sulfur deposition in sour gas wells. World Oil **1983**, *35*.

(2) Chesnoy, A. B.; Pack, D. J. Acid gas injection eliminates sulfur recovery expense. *Oil Gas J.* **1997**, *95/17*, 74–78.

(3) Wilkes, C.; Pareek, V. *Energy-Tech Online*, 2001 (accessed March 2008).

(4) Pack, D. J., Paper presented at the 14th Biennal Joint Technical Meeting on Pipelines Research, Berlin, 2003, paper no 31, 1−14.

(5) Rau, H.; Kutty, T. R. N.; Guedes de Carvalho, J. R. F. Thermodynamics of sulphur vapour. *J. Chem. Therm.* **1973**, *5/6*, 833–844.

(6) Rau, H.; Kutty, T. R. N.; Guedes de Carvalho, J. R. F. High temperature saturated vapour pressure of sulphur and the estimation of its critical quantities. *J. Chem. Therm.* **1973**, *5/2*, 291–302.

(7) Lenain, P.; Picquenard, E.; Corset, J. *Ber. Bunsen. Phys. Chem.* **1988**, *92*, 859–870.

(8) Steudel, R.; Steudel, Y.; Wong, M. W. Specification and thermodynamics of sulfur vapor. *Top. Curr. Chem.* **2003**, *230*, 117–134.

(9) Serin, J. P.; Cézac, P.; Broto, F.; Mouton, G. Modelling of sulphur deposition in natural gas. *Comput.-Aided Chem. Eng.* **2005**, *20/1*, 799–804.

(10) Cézac, P.; Serin, J. P.; Mercadier, J.; Mouton, G. Modelling solubility of solid sulphur in natural gas. *Chem. Eng. J.* **2007**, *133*, 283–291.

(11) Cézac, P.; Serin, J. P.; Reneaume, J. M.; Mercadier, J.; Mouton, G. Elemental sulphur deposition in natural gas transmission and distribution networks. *J. Supercrit. Fluids* **2008**, *44/2*, 115–122.

(12) Serin, J. P.; Cézac, P. Three thermodynamic paths to describe solid fugacity: Application to sulphur precipitation from supercritical natural gas. *J. Supercrit. Fluids* **2008**, *46/1*, 21–26.

(13) Hyne, J. B.; Muller, E.; Wiewiorowski, T. K. Nuclear magnetic resonance of hydrogen polysulfides in molten sulfur. *J. Phys. Chem.* **1966**, *11*, 3733–3735.

(14) Karan, K.; Heidemann, R. A.; Behie, L. A. Sulfur solubility in sour gas: predictions with an equation of state model. *Ind. Eng. Chem. Res.* **1998**, *37/5*, 1679–1684.

(15) Berkowitz, J. *Elemental Sulfur*; Meyer, B., Ed.; Interscience, John Wiley & Sons: New York, 1965; pp 125−159.

(16) Heidemann, R. A.; Phoenix, A. V.; Karan, K.; Behie, L. A. A chemical equilibrium equation of state model for elemental sulfur and sulfur-containing fluids. *Ind. Eng. Chem. Res.* **2001**, *40/9*, 2160–2167.

(17) MacKnight, W. J.; Tobolsky, A. V. *Elemental Sulfur*; Meyer, B., Ed.; Interscience, John Wiley & Sons: New York, 1965; pp 95−107.

(18) Rivollet, F. Etude des propriétés volumétriques (PVT) d'hydrocarbures légers (C1-C4), du dioxyde de carbone et de l'hydrogène sulfuré: Mesures par densimétrie à tube vibrant et modélisation. (Study of volumetric properties (PVT) of light hydrocarbons (C1-C4), carbon dioxide, and hydrogen sulfide: Measurements by densimetric tube and vibrant model.) Ph.D. Thesis. Paris School of Mines, France, 2005 (in French).

(19) Wilamowski, B.; Iplikci, S.; Kayank, O.; Efe, M. O. International Joint Conference on Neural Networks (IJCNN'01), Washington, DC, 15−19 July 2001, pp 1778−1782.

(20) Marquardt, D. An algorithm for least-squares estimation of nonlinear parameters. *SIAM J. Appl. Math.* **1963**, *11*, 431–441.

(21) Levenberg, K. A method for the solution of certain problems in least squares. *Quart. Appl. Math.* **1944**, *2*, 164–168.

(22) Normandin, A.; Grandjean, B. P. A.; Thibault, J. PVT data analysis using neural network models. *Ind. Eng. Chem. Res.* **1993**, *32*, 970–975.

(23) Kennedy, H. T.; Wieland, D. R. Equilibrium in the methane-carbon dioxide-hydrogen sulfide system. *Pet. Trans. AIME* **1960**, *219*, 166–169.

(24) Roof, J. G. Solubility of sulfur in hydrogen sulfide and in carbon disulfide at elevated temperature and pressure. *Soc. Pet. Eng. J.* **1971**, *272*, 276.

(25) Brunner, E.; Woll, W. Solubility of sulfur in hydrogen sulfide and sour gases. *Soc. Pet. Eng. J.* **1980**, *377*, 384.

(26) Tomcej, R. A.; Kalra, H.; Hunter, B. E. Prediction of Sulphur Solubility in Sour Gas Mixtures. Presented at the 39th Annual Technical Meeting of the Petroleum Society of CIM, Calgary, Alberta, 12 June 1988; Paper No. 88−39−14.

(27) Swift, S. C.; Manning, F. S.; Thompson, R. E. Sulfur-bearing capacity of hydrogen sulfide gas. *Soc. Pet. Eng. J.* **1976**, *57*, 64.

(28) Brunner, E.; Place, M. C.; Woll, W. H. Sulfur solubility in sour gas. *J. Pet. Tech.* **1988**, 1587–1592.

(29) Woll, W. The influence of sour gases upon the melting curve of sulfur. *Erdoel-Erdgas-Z.* **1983**, *99*, 297.

(30) Davis, P. M.; Lau, C. S. C.; Hyne, J. B. Data on the solubility of sulfur in sour gases. Alberta Sulphur Res. Ltd. Q. Bull. **1992−1993**, *24*, 1.

(31) Gu, M. X.; Li, Q.; Zhou, Sh.Y.; Chen, W. D.; Guo, T. M. Experimental and modeling studies on the phase behavior of high H2S-content natural gas mixtures. *Fluid Phase Equilib.* **1993**, *82*, 173–182.

(32) Migdisov, A. A.; Suleimenov, O. M.; Alekhin, Y. V. Experimental study of polysulfane stability in gaseous hydrogen sulfide. *Geochim. Cosmochim. Acta* **1998**, *62*, 2627.

(33) Sun, C. Y.; Chen, G. J. Experimental and modelling studies on sulfur solubility in sour gas. *Fluid Phase Equilib.* **2003**, *214*, 187–195.

(34) Peng, D. Y.; Robinson, D. B. A new two-constant equation of state. *Ind. Eng. Chem. Fundam.* **1976**, *15/1*, 59–64.

(35) Chouai, A.; Laugier, S.; Richon, D. Modeling of thermodynamic properties using neural networks application to refrigerants. *Fluid Phase Equilib.* **2002**, *199*, 53–62.

(36) Piazza, L.; Scalabrin, G.; Marchi, P.; Richon, D. Enhancement of the extended corresponding states techniques for thermodynamic modelling. I. Pure fluids. *Int. J. Refrig.* **2006**, *29/7*, 1182–1194.

(37) Scalabrin, G.; Marchi, P.; Bettio, L.; Richon, D. Enhancement of the extended corresponding states techniques for thermodynamic modelling. II. Mixtures. *Int. J. Refrig.* **2006**, *29/7*, 1195–1207.

(38) Chapoy, A.; Mohammadi, A. H.; Richon, D. Predicting the hydrate stability zones of natural gases using artificial neural networks. *Oil Gas Sci. Technol.—Rev. IFP* **2007**, *62/5*, 701–706.

Received for review March 18, 2008
Revised manuscript received June 16, 2008
Accepted August 12, 2008

IE8004463